Indian Journal of Chemical Technology
Vol. 23, September, 2016 pp. 374-383

Removal of arsenic from aqueous solution by an adsorbent nickel ferrite-polyaniline nanocomposite

Sonal Agrawal & N B Singh*

Research and Technology Development Centre Sharda University, Greater Noida 201 306, India
E-mail: nbsingh43@gmail.com

Received 16 December 2015; accepted 6 May 2016

Nickel ferrite-polyaniline nanocomposite has been prepared and characterized using different techniques. The prepared nanocomposite is used as an adsorbent for the removal of arsenic from aqueous solution of sodium arsenite. The effect of temperature on the equilibrium adsorption of As(III) from aqueous solution on nanocomposite has been investigated. Effect of *p*H (2-12), contact time (0-70 min), adsorbent dose (0.1-0.8) and initial metal ion concentration (10-30 mg/L) on the removal of As (III) have been studied. The maximum removal efficiency is found at *p*H 8.0. It is found that nickel ferrite-polyaniline is a better adsorbent for removal of As(III) as compared to many others. The Langmuir adsorption isotherm model fits the data well and the process is found to be pseudo-second order. In order to understand the adsorption process, thermodynamic parameters such as $\Delta G°$, $\Delta H°$, and $\Delta S°$, have been calculated.

Keyword: Neckel ferrite, Nanocomposite, Arsenic, Adsorption, Langmuir isotherm

Water plays a vital role in the smooth functioning of the earth's ecosystem. Presence of heavy metals particularly As(III) in water have adverse effect on the ecosystem and affects millions of people across the globe[1]. The sources of arsenic in ground water are primarily associated with oxidative weathering but other sources are due to anthropogenic activities such as industrial effluents from metal processing and agriculture activities such as fertilizers and pesticides, glass and ceramics industries and medicinal activities, and discharges from chemical processing/manufacturing plants[2]. In water arsenic exists primarily as arsenate, As(V), and arsenite, As(III). The arsenic species which predominates depend on the *p*H of the solution. The most dominant species in natural water are given by Eqns 1–3 (Ref. 3).

$$H_3AsO_4 \Leftrightarrow H^+ + H_2AsO_4^- \quad pK_1 = 2.2 \qquad \ldots(1)$$

$$H_2AsO_4^- \Leftrightarrow H^+ + HAsO_4^{2-} \quad pK_2 = 6.9 \qquad \ldots(2)$$

$$HAsO_4^{2-} \Leftrightarrow H^+ + AsO_4^{3-} \quad pK_3 = 11.5 \qquad \ldots(3)$$

It is reported that arsenic (III) is more toxic and stable than arsenic (V) because of electronic configuration[4]. Long term ingestion of arsenic contaminated drinking water causes kidney, lungs and skin cancer, gastrointestinal disease, bone marrow disorder, cardiovascular diseases and other diseases[5-8]. Due to extreme toxicity of arsenic, the maximum permissible limit of arsenic in drinking water set by World Health Organization (WHO, Geneva, Switzerland), Environmental Protection Agency (US-EPA, United States)[9-10] and Central Pollution Control Board (CPCB, India)[11,12] is 0.01 to 0.05 mg L^{-1}.

There are number of methods for the removal of arsenic from water (Fig. 1)[13-18]. Among the mentioned technologies, adsorption is inexpensive, simple in operation and applicable at different scales ranging from small units for household users to large industrial plants[19].

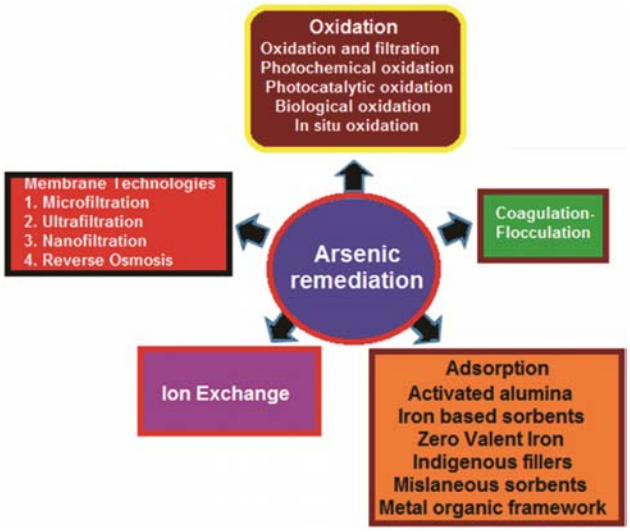

Fig. 1 — Different methods of water purification

Various type of adsorbents have been used for removal of arsenic from water. Some important adsorbents are agricultural biomass, activated carbon, resins, sand, zirconium oxides, iron and alumina based adsorbents[20-23]. The major problems of these adsorbents are their separation, poor adsorption efficiency, and low recyclability. Recent advances in nanotechnology offer better alternative for water purifications[24].

In recent years a large number of nanomaterials have been used as adsorbents to remove heavy metals, dyes, synthetic organic chemicals etc. from aqueous solutions. They have been suggested as a cost effective and environment friendly adsorbent for the removal of toxic elements from aqueous solution[25,26]. Fe_2O_3, Fe_3O_4, TiO_2, Al_2O_3 etc. of nanodimensions are found to be more promising adsorbents because of their large surface area and porous structure[27]. Application of iron oxide based nanomaterial is more attractive for removal of heavy metals contamination from the water because of their important features like small size, high surface area, and magnetic properties[28,29]. Number of ferrites (magnetic nanoparticles) such as $MnFe_2O_4$, $CoFe_2O_4$, $ZnFe_2O_4$, $CuFe_2O_4$, $NiFe_2O_4$, and $MgFe_2O_4$ have also been used as adsorbents for purification of water[26]. Among various ferrites, nickel ferrite ($NiFe_2O_4$) is a inverse spinel, where Fe^{3+} ions are located in the tetrahedral and octahedral sites and Ni^{2+} ions are located in octahedral sites only[30]. Powder of nanosized nickel ferrite is a useful material due to its high electromagnetic performance, excellent chemical stability and mechanical hardness, high coercivity, and moderate saturation magnetization. These unique properties of nickel ferrite made it a good candidate for various applications[30].

Magnetic property of iron oxide nanaparticles enables easy separation of adsorbents from the system. These particles are capable of removing pollutants even at low concentration under varied conditions of *p*H and temperature[26]. The dose of nanoparticles required is quite low, making their application economical. However the major drawbacks with nanoparticles are their agglomeration, health and environmental issues.

In order to minimize these problems, polymeric nanocomposites have been used as adsorbents for the removal of toxic metal ions from wastewater[31]. The properties of $NiFe_2O_4$ and its nanocomposite with polyaniline have been studied[32] but their use for removal of arsenic from water has not been reported.

Recently we used $NiFe_2O_4$ – PANI nanocomposite as an adsorbent for removal of chromium (III) from water system and found very effective[33]. In the present investigation nickel ferrite-polyaniline ($NiFe_2O_4$ – PANI) nanocomposite has been prepared, characterized and used as an adsorbent for the removal of arsenic from aqueous solution containing trace amounts. The effect of experimental parameters such as contact time, solution *p*H, adsorbent dose, temperature etc on the removal of arsenic has been studied. Adsorption isotherms and a possible mechanism of adsorption have been discussed.

Experimental Section

Materials

Nickel sulphate (Fisher Scientific), ferric nitrate (Qualikems), ammonia solution, sodium hydroxide, sodium arsenite, aniline (Lobachemie), benzene (Fisher Scientific) and copper sulphate (Qualigens) were used. Solutions of the reagents were prepared in distilled water.

Preparation of $NiFe_2O_4$

Water solutions of nickel sulphate and ferric nitrate were mixed in 1:2 molar ratio. Mixing was continued till a clear solution was obtained. Ammonium hydroxide solution was added to this solution till Nickel hydroxide and Ferric hydroxide co- precipitated. The precipitate thus obtained was washed with water, dried and calcined at 300°C/500°C for 3h, where nanosize $NiFe_2O_4$ was obtained.

Preparation of polyaniline and *$NiFe_2O_4$-PANI- nanocomposite*

First of all PANI was prepared by oxidation of aniline. Aniline was mixed with benzene at room temperature and stirred magnetically to have 0.1 M solution. 0.1 M $CuSO_4$ solution was added drop by drop to the aniline solution and continuously stirred for 30 min, where polymerization of aniline took place and PANI was formed. Secondly during polymerization process (in situ) 5.0 wt% $NiFe_2O_4$ was mixed thoroughly using magnetic stirrer for 30 minutes where $NiFe_2O_4$-PANI nanocomposite was formed. The nanocomposite formed was washed with hot water and dried at 80°C for 2h for removal of adsorbed water and stored in a desiccator.

Characterization

Powder X-ray diffraction (XRD) pattern of $NiFe_2O_4$, PANI and 5% $NiFe_2O_4$ – PANI were recorded with the help of X – ray diffractometer using CuK_α radiation.

TG studies of PANI and $NiFe_2O_4$-PANI nanocomposite were studied in N_2 atmosphere from room temperature to 1173 K.

The FTIR spectra of $NiFe_2O_4$-PANI and PANI films were recorded with a spectrometer (model Shimadzu IR-Affinity-1) at room temperature with NETZSCH STA 409 PC LUXX.

ESEM images of $NiFe_2O_4$, $NiFe_2O_4$- PANI and PANI were obtained from Quanta FEG 250ESEM.

The electrical conductivities of PANI and $NiFe_2O_4$ - PANI nanocomposite were measured by a.c. impedance spectroscopic method using Hioki 3532-50 LCR Hi Tester.

Removal of arsenic from aqueous solution

UV – visible spectra of sodium arsenite solution of different concentrations in water were recorded with the help of spectrophotometer and λ_{max} 560 nm was found out. The initial *p*H of the arsenite solution under investigation was about 12.0. Calibration curve was made. 0.2 g of $NiFe_2O_4$-PANI nanocomposite was dispersed in 10 mL of 10 ppm arsenic solution kept in 10 test tubes and each was slowly stirred magnetically. After every 10 min, the absorbance of the arsenic solution was recorded at λ_{max} = 560 nm and the concentrations determined. Similar experiments were done with PANI alone. Experiments were performed at different *p*H (2-12). 0.1 N NaOH/0.1 N HCl solutions were used to adjust the *p*H of the solution. The adsorption of arsenic on the surface of $NiFe_2O_4$ - PANI nanocomposite was studied as a function of time (0-70 min) and adsorbent dose. The percentage removal of arsenic was estimated using Eq(4)[34]:

$$\text{Removal } \% = \frac{C_o - C_e}{C_o} \times 100 \quad \ldots(4)$$

where C_o and C_e are the initial and the equilibrium concentrations of arsenic respectively in mg/L. The effect of nanocomposite dosage on adsorption of arsenic was examined by varying the mass of adsorbent from 0.1 to 0.8 g. The initial concentration of arsenic was 10 ppm. The sample volume was 10 mL.

Adsorption experiments were performed at 288, 298 and 308 K and *p*H 12.0. The equilibrium sorption capacity was determined using Eq.(5):

$$q_e = \frac{(C_o - C_e)V}{m} \quad \ldots(5)$$

where q_e is the equilibrium amount of arsenic adsorbed per unit mass of the adsorbent (mg/g) and V is the sample volume (mL) and m is the mass of the adsorbent dosage in (g). From the data, thermodynamic parameters (ΔG^0, ΔH^0 and ΔS^0) were calculated. Adsorption kinetics was studied by mixing 0.20 g of adsorbent with 10 mL of arsenic solution at room temperature (25°C). The amount of arsenic adsorbed was calculated using Eq.(6):

$$q_t = \frac{(C_o - C_t)V}{m} \quad \ldots(6)$$

where q_t is the time-dependent amount of arsenic adsorbed per unit mass of adsorbent (mg/g), C_t is the bulk-phase arsenic concentration (mg/L) at any time t and m is the adsorbent mass (g).

Results and Discussion

Preparation of $NiFe_2O_4$-PANI nanocomposite

The formation of Nickel ferrite is represented by Scheme 1.

PANI was formed as shown in Scheme 2 (Ref 35). In situ polymerization gave $NiFe_2O_4$ –PANI nanocomposite. The formation of nanocomposite is shown in Scheme 3.

Characterization of $NiFe_2O_4$-PANI nanocomposite

Figure 2 gives the XRD pattern of $NiFe_2O_4$, polyaniline and $NiFe_2O_4$ – PANI nanocomposite. The characteristic peaks of $NiFe_2O_4$ with reflection of Fd3m cubic spinel group (PDF 10-0325), correspond to a single-spinel phase[36]. The broadening of the diffraction peaks suggested that the prepared

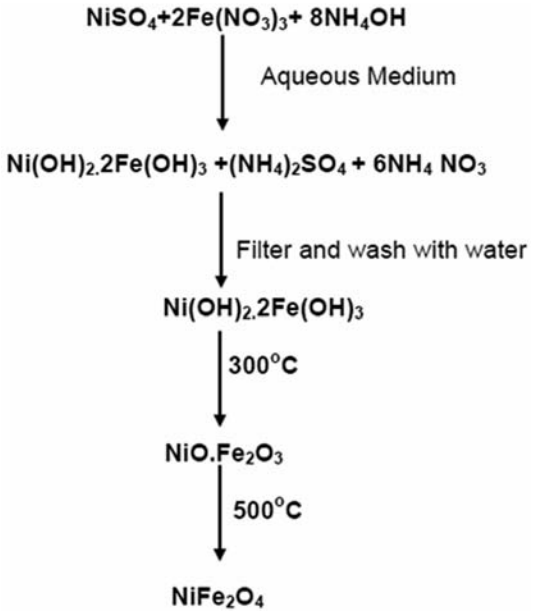

Scheme 1 — Preparation of $NiFe_2O_4$

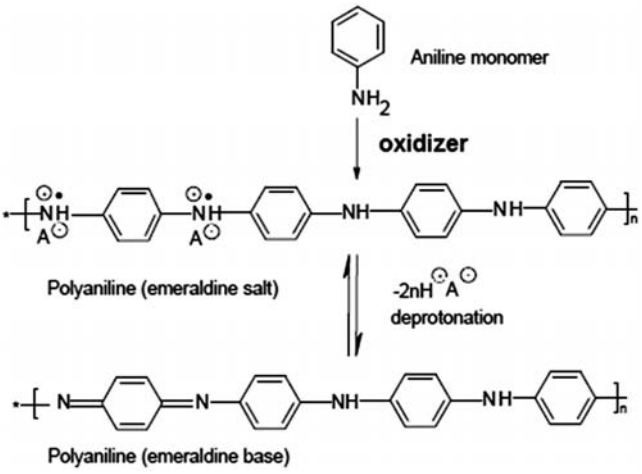

Scheme 2 — Formation of polyaniline from aniline and its two forms

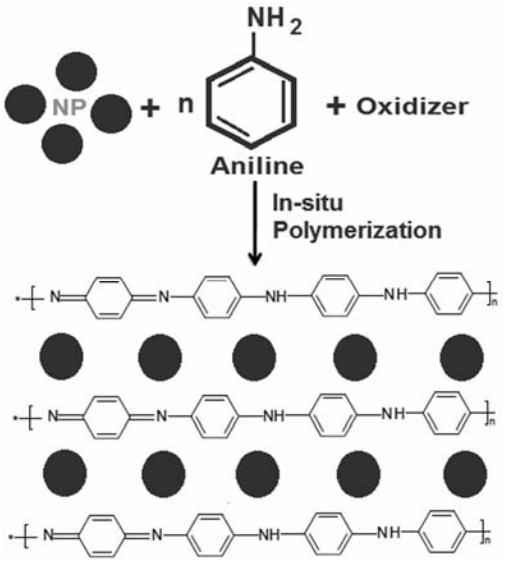

Scheme 3 — Preparation of $NiFe_2O_4$ – PANI nanocomposite

sample is very small in dimensions. The crystallite size D was calculated from XRD peak broadening of the (311) peak using Debye–Scherrer formula: $D = 0.9\lambda/\beta \cos\theta$, where D is the average crystallite size, λ is the wavelength of CuK_α radiation, β is the full width at half maximum (FWHM) of the diffraction peaks and θ is the Bragg's angle. The crystallite size of $NiFe_2O_4$ was found approximately 27-35 nm. PANI gave peaks at 2θ =, 20^o, 27^o which may be due to the periodicity parallel and perpendicular to PANI chains, respectively[37]. In the XRD pattern of $NiFe_2O_4$–PANI nanocomposite, the peak intensities of PANI are decreased indicating the formation of $NiFe_2O_4$–PANI nanocomposite.

Thermo gravimetric analyses showed that the thermal stability of the nanocomposites was much

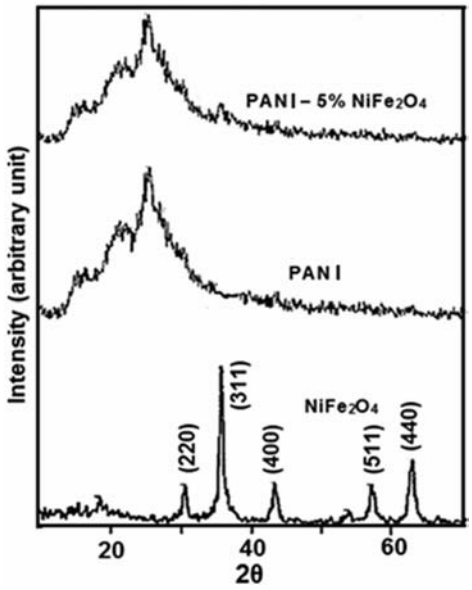

Fig. 2 — X-ray diffraction patterns of $NiFe_2O_4$, polyaniline and $NiFe_2O_4$ – PANI nanocomposite

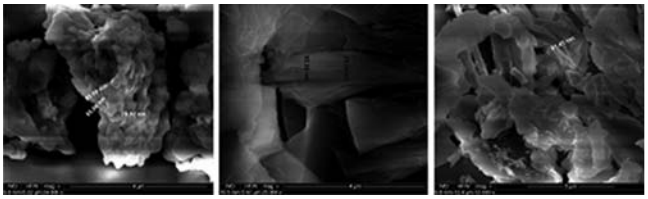

Fig. 3 — SEM pictures of $NiFe_2O_4$, PANI and $NiFe_2O_4$-PANI

higher than that of pure PANI. This may be due to the interaction between ferrite particles and PANI chains.

FTIR spectral studies showed that the vibrational frequencies of PANI are shifted in the case of $NiFe_2O_4$–PANI nanocomposite showing that there are some interactions between PANI chains and nickel ferrite particles.

SEM pictures of $NiFe_2O_4$, PANI and $NiFe_2O_4$-PANI are shown in Fig. 3. The particle size of $NiFe_2O_4$ is about 30-35 nm indicating that $NiFe_2O_4$ is a nanomaterial. SEM picture of PANI indicates a flaky structure whereas $NiFe_2O_4$-PANI has a homogeneous flaky structure. SEM pictures thus indicated the formation of homogeneous $NiFe_2O_4$-PANI nanocomposite.

Electrical conductivity measurements have indicated that there was a slow increase in electrical conductivities of PANI with temperature. However, in the case of $NiFe_2O_4$-PANI nanocomposite, the electrical conductivity values were almost constant and lower than that of PANI in the temperature range studied. It is reported that the ferrite particles in $NiFe_2O_4$-PANI nanocomposite is insulator that's

why conductivity of $NiFe_2O_4$-PANI nanocomposite was almost constant with increasing temperature[38]. The lower value of electrical conductivity of $NiFe_2O_4$-PANI may be due to partial blockage of the conducting path in PANI matrix by insulating ferrite particles[39,40]. The variation of electrical conductivity with frequency was also studied. The conductivity of $NiFe_2O_4$-PANI nanocomposite increased as the frequency increased. The variation of conductivity with frequency may be due to interface charge polarization and intrinsic electric dipole polarization[41]. The dielectric properties of polymer composites depend on several factors including the size and filler content as well as the interfacial bonding between the filler and polymer matrix. The dielectric constant decreased with frequency and was higher for PANI at all the frequencies. The dipole can respond rapidly at lower frequency to follow the field so the highest dielectric constant. The dipole polarizability will be lower at higher frequencies, as the field cannot induce the dipole moment, so the dielectric values attain the minimum. The lower values of dielectric constant in the case of $NiFe_2O_4$-PANI nanocomposite may be due to interfacial and space charge polarization.

Arsenic removal from aqueous solution of sodium arsenite

Effect of contact time on adsorption

Contact time and initial concentration have significant effects on the removal of arsenic from aqueous solution. The adsorption of arsenic on $NiFe_2O_4$-PANI nanocomposite was studied as a function of time and arsenic concentration (10, 20 and 30 mg/L). Figure 4 shows that the adsorption increased with time and initial arsenic concentration. Percent removal of arsenic in the presence of PANI is found to be much lower as compared to that of $NiFe_2O_4$-PANI nanocomposite.

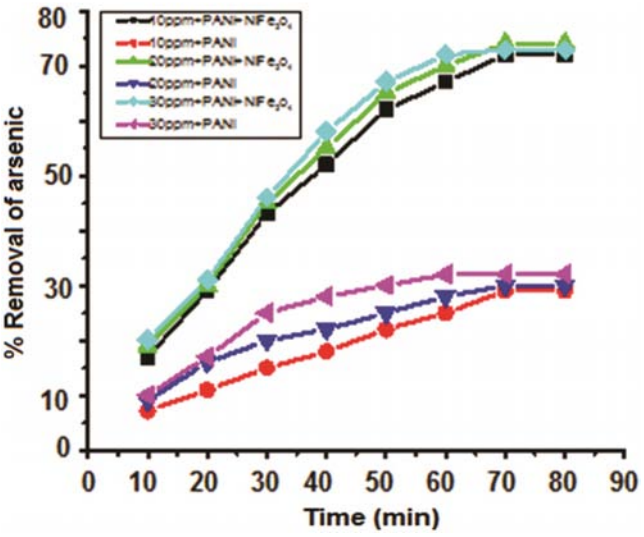

Fig. 4 — Removal of Arsenic with time in the presence of PANI and $NiFe_2O_4$-PANI at different concentration of arsenic

Effect of pH on adsorption

Oxidation states of the metals in solutions are *p*H dependent.[34] Arsenic adsorption is also known to be *p*H-dependent, moreover, the surface groups of the adsorbent are considered vulnerable to be protonated and deprotonated. Chemical speciation of the metal ions as well as the ionization of the functional groups onto the adsorbent surfaces are also *p*H dependent[42,43]. In general As(III) and As(V) coexist in ground water and there are significant differences in their chemical behavior. The dissociation reactions and the corresponding equilibrium constants of H_3AsO_4 and H_3AsO_3 are given in Table 1 (Ref 44).

The non-dissociated As(III) exists in slightly acidic or neutral medium. Below *p*H = 8, considerable amount of anionic species have been reported. However, As(V) exists as completely dissociated in the form of monovalent, divalent and trivalent anions. The speciation diagrams of As(V) and As(III), are shows in Figs. 5(a) and (b) respectively.[45]

Percent removal of arsenic increased upto *p*H 8 and after that decreased. The results showed that in acidic medium the adsorption capacity of nanocomposite increased with increase of *p*H (decrease of acid character). However in basic medium the adsorption capacity decreased with increase of *p*H of the solution. The arsenic adsorption could be affected by the surface property of the adsorbent and the existing species of the adsorbate, which are both *p*H-dependent. H_3AsO_3 has a *p*Ka of 9.2, and at *p*H below 9.2, As(III) is mainly present as neutral H_3AsO_3, while at *p*H above 9.2, $H_2AsO_3^-$ dominates[46]. Iron oxides possess surface hydroxyl groups, which can be protonated or deprotonated in solution depending on the *p*H[47].The results suggest that highly protonated or weakly protonated surfaces are not favourable for

Table 1—Dissociation constants of arsenate and arsenite[41]

Speciation	Dissociation reactions	pK_a
As(V)	$H_3AsO_4 \leftrightarrow H^+ + H_2AsO_4^-$	2.24
	$H_2AsO_4^- \leftrightarrow H^+ + H_2AsO_4^{2}$	6.69
	$H_2AsO_4^{-2} \leftrightarrow AsO_4^{3-}$	11.5
As(III)	$H_3AsO_3 \leftrightarrow H^+ + H_2AsO_3^-$	9.2
	$H_2AsO_3^- \leftrightarrow H^+ + H_2AsO_3^{2-}$	12.1
	$H_2AsO_3^{-2} \leftrightarrow AsO_3^{3-}$	13.4

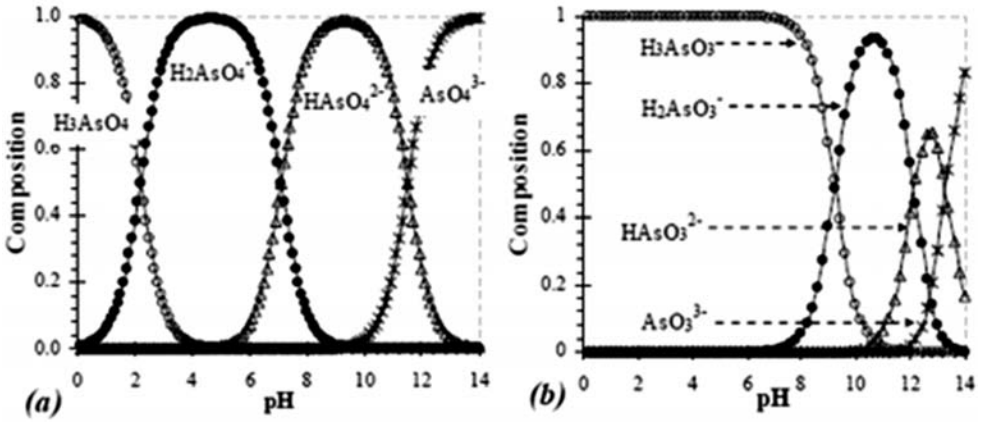

Fig. 5 — Speciation diagram of (a) As(V) and (b) As (III)

adsorption[48]. It appears that electrostatic attraction may not be the major mechanism of adsorption of arsenate on the surface of nanocomposite.

Effect of adsorbent dosage on adsorption

The percentage removal of arsenic was studied by varying the adsorbent dose from 0.1-0.8g/10 mL of 10 ppm solution. The arsenic removal efficiency increased up to an optimum dosage (0.7 g) beyond which the removal efficiency did not significantly change. The removal efficiency was much higher for the nanocomposite. Increase in adsorption with adsorbent dosage can be attributed to the availability of more adsorption sites because of higher surface area. It appears that at concentration of 10 ppm, the whole surface of adsorbent was covered with the adsorbate and there was no free surface left for adsorption. Therefore, 0.7g of adsorbent became the optimum amount for 10 ppm concentration of adsorbate.

Adsorption Isotherm

Langmuir and Freundlich adsorption isotherm models were used to examine the isotherm data. The Langmuir isotherm model is given by Eq. (7) and its validity is shown in (Fig. 6).

$$\frac{1}{q_e} = \frac{1}{q_m b c_e} + \frac{1}{q_m} \qquad \ldots(7)$$

where C_e (mg/L) and q_e (mg/g) are the equilibrium concentration of adsorbate in liquid phase and on the solid phase, respectively. b (L/mg) is Langmuir constant related to binding energy of the adsorbent and q_m (mg/g) the theoretical monolayer coverage of adsorbate on the adsorbent.

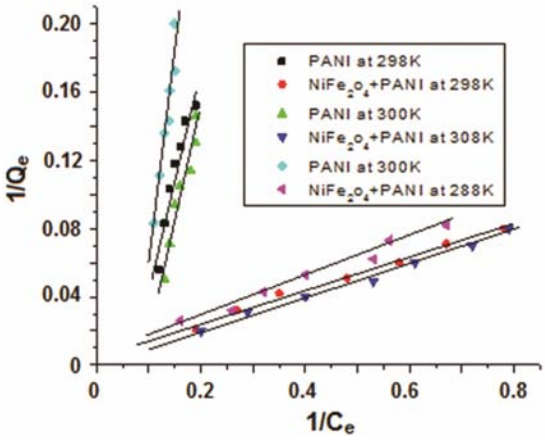

Fig. 6 — Verification of Langmuir adsorption Isotherm (Eq.4)

Langmuir isotherm model for gases on solids is based on a monolayer adsorption. Molecules of adsorbate do not deposit on other adsorbate molecules already adsorbed. However, in solution-solid systems, the process is much more dynamic and complicated. In such systems the isotherm adequacy can be seriously affected by the experimental conditions, in particular, the range of concentration of the solute/adsorbate as well as *p*H and temperature.

The important characteristic of Langmuir isotherm, called dimensionless separation factor (R_L), is defined by Eq. (8). The values of R_L were 0.568, 0.285 and 0.537 respectively at 288K, 298K and 308K in case of PANI, where the values of R_L were 0.653, 0.709 and 0.909 respectively at 288K, 298K and 308K respectively in case of $NiFe_2O_4$-PANI, indicating that adsorption is favourable in both the cases:

$$R_L = \frac{1}{1 + b c_o} \qquad \ldots(8)$$

Favorable adsorption is suggested if the value of R_L lies in the range $0 < R_L < 1$. The adsorption is unfavorable if $R_L > 1$ and $R_L = 1$ indicates linear adsorption while $R_L = 0$ suggests irreversible nature of adsorption process. Since in the present case the value of R_L is less than 1, adsorption on the surface of adsorbent is favorable. However, the value of R_L was higher for $NiFe_2O_4$-PANI nanocomposite as compared to PANI.This indicated that adsorption of arsenic on $NiFe_2O_4$-PANI nanocomposite is more favorable and increased with temperature.

Freundlich adsorption isotherm is given by Eq. (9) which is valid for multilayer adsorption.

$$\log q_e = \log K_F + \frac{1}{n}\log C_e \qquad \ldots(9)$$

where K_F is a Freundlich constant and defined as the adsorption or distribution coefficient, related to the binding energy, n is Freundlich constant and is a measure of the adsorption intensity or surface heterogeneity. The validity of Eq (9) was tested by plotting a graph between $\log q_e$ and $\log C_e$.

The Langmuir and Freundlich isotherm parameters were calculated and are given in Table 2. The higher values of correlation coefficient (R^2) revealed that Langmuir model fitted well the isotherm data compared to the Freundlich model. Extent of adsorption of As(III) on different adsorbents as reported in the literature are given in Table 3. Since the values are at different *p*H, it is difficult to compare. However, in general $NiFe_2O_4$-PANI nanocomposite is found to be a better adsorbent for As(III) removal from water solution.

Sorption kinetics

Adsorption kinetics gives important information concerning the mechanism of adsorption and allows comparing different adsorbent under distinct operational conditions for similar applications[62]. It was found that arsenic adsorption approached to equilibrium within 60 min. To understand the kinetics of the adsorption process, kinetic models such as pseudo-first-order and pseudo-second-order models were tested. The linearized forms of the pseudo-first order and pseudo-second-order processes are given by Eqs. (10) and (11), respectively:

$$\log (q_e - q_t) = \log q_e - \left(\frac{k_1}{2.303}\right)t \qquad \ldots(10)$$

$$\frac{t}{q_t} = \frac{1}{k_2 q_e^2} + \frac{t}{q_e} \qquad \ldots(11)$$

where q_t is arsenic uptake at time t, and k_1 and k_2 are the pseudo first order and second order rate constants, respectively. The validity of Eq. (10) was tested by plotting log (q_e-q_t) against time, where straight lines are obtained. In order to test the validity of Eq.(11), t/q_t was plotted against t, where straight lines were obtained. From the plots, the rate constants were determined and are given in Table 4. The correlation coefficients R^2 were also calculated and are given in Table 4. Higher values of correlation coefficient indicated that the pseudo-second-order model fitted the data for arsenic adsorption. It appears that only monolayer adsorption of arsenic occurs at the surface of the adsorbent.

Thermodynamic parameters

Thermodynamic considerations of an adsorption process are necessary to know whether the process is spontaneous or not. Experiments were performed at different temperatures and the thermodynamic parameters such as free energy (ΔG^0), enthalpy (ΔH^0) and entropy (ΔS^0) changes for adsorption were calculated[63]. The van't Hoff equation (Eq.12) was used to determine the value of the equilibrium constant

$$\frac{d(1nK)}{dT} = \frac{\Delta H^0}{RT^2} \qquad \ldots(12)$$

Table-2 — Langmuir and Freundlich Isotherm parameters for arsenic adsorption onto $NiFe_2O_4$-PANI nanocomposite and PANI

Adsorbent	$NiFe_2O_4$-PANI						PANI					
temp(K)	Freundlich Isotherm			Langmuir Isotherm			Freundlich Isotherm			Langmuir Isotherm		
	1/n	K	R^2	Qm	b	R^2	1/n	K	R^2	Qm	b	R^2
288	0.844	8.81	0.97	166.6	0.053	0.98	2.42	0.057	0.92	5.29	0.076	0.92
298	0.919	9.84	0.98	250	0.042	0.99	2.20	0.137	0.89	25.6	0.254	0.94
308	0.976	10.23	0.97	1000	0.010	0.98	2.28	0.158	0.94	8.84	0.086	0.93

Table.3—Langmuir and Freundlich Isotherm parameters for arsenic adsorption onto $NiFe_2O_4$-PANI nanocomposite and PANI

Adsorbents	Equilibrium concentration (mg/L)	Solution *p*H	Sorption capacity (mg/g)	Ref.
Nanocrystalline TiO2	0.6	7.0	8.3	[48]
Powder Ce–Ti sorbent	0.01	6.5	6.8	[49]
Granular Ce–Ti sorbent	0.01	6.5	0.9	[49]
Activated alumina	0.1	7.6	0.08	[50]
Fe–Mn binary oxide	0.75	5.0	73.5	[51]
MnO2-loaded resin	3	7.0-8.5	26	[52]
Zr-loaded resin	0.14	9.0	29.2	[53]
Polyaniline/polystyrene nanocomposite	0.25-1	8.0	52	[54]
Nickel/nickel boride nanoparticles	0.25	3.3-11.5	23.4	[55]
Neolitic imidazolate framework-8	0-100	7.0	49.49	[56]
Iron–chitosan flakes	1-10	7.0	16.15	[57]
CuO nanoparticles	0.1-100	8.0	26.9	[58]
Fe_3O_4	0-100	7.0	5.68	[59]
Nanosize zerovalent iron/Activated carbon	2	6.5	18.2	[60]
Polyaniline(PANI)	10-30	8.0	25.2	This study
$NiFe_2O_4$-PANI	10-30	8.0	25	This study

Table 4 — Kinetic parameters for arsenic adsorption onto PANI-$NiFe_2O_4$ nanocomposite and PANI

C_0 (mg/L)	Adsorbent	Pseudo-first-order kinetics			Pseudo-second-order kinetics		
		k_1 (1/min)	q_e (mg/g)	R^2	k_2 (g/mg min)	q_e (mg/g)	R^2
10	$NiFe_2O_4$-PANI	0.0529	2.69	0.917	0.00003	333.3	0.999
10	PANI	0.0414	2.19	0.936	0.00001	1000	0.925

The equilibrium constant is expressed by Eq. (13)[64,65]:

$$K = \frac{q_e}{C_e} \quad ...(13)$$

The Gibbs free energy is given by Eq. 14.

$$\Delta G^0 = \Delta H^0 - T\Delta S^0 \quad ...(14)$$

The free energy change is related to equilibrium constant by Eqn.(15)

$$\Delta G^0 = -RT \ln K \quad ...(15)$$

These equations are combined to obtain

$$\ln K = \frac{\Delta S^0}{R} - \frac{\Delta H^0}{RT} \quad ...(16)$$

Once the values of enthalpy (ΔH^0) and entropy (ΔS^0) were determined, the value of ΔG^0 is determined by Eq. (14). The enthalpy and entropy changes of the adsorption process were calculated from the slope and intercept of line obtained by plotting ln K against 1/T. The calculated values of ΔG^0, ΔH^0 and ΔS^0 are given in Table 5.

Gibb's free energy change, $\Delta G°$, is the fundamental criteria of spontaneity. Adsorption on the surface of nanocomposite occurs spontaneously at a given temperature because $\Delta G°$ is negative (Table 5). The decrease in the value of $\Delta G°$ with an increase in temperature indicated that the adsorption process of As (III) on $NiFe_2O_4$-PANI nanocomposite is more favorable at higher temperatures[66]. The positive value of $\Delta H°$ indicated that the adsorption reaction is endothermic, as a result of which the adsorption efficiency increased with the increase of temperature[67]. Entropy has been defined as the disorderness of a system. The positive value of $\Delta S°$ suggested that some structural changes occured on the surface of adsorbent, and the randomness at the solid/liquid interface in the adsorption system increased during the adsorption process.

Table.5 — Thermodynamic parameters for arsenic adsorption onto PANI/$NiFe_2O_4$ nanocomposite

Adsorbent	ΔS^0(J mol^{-1} $K^{-1)}$	ΔH^0 (J $mol^{-1)}$	ΔG^0 (J $mol^{-1)}$ at different temperatures		
			288 K	298 K	308 K
$NiFe_2O_4$-PANI	41.57	83140	-6932.16	-9893.6	-12219.59
PANI	-33.25	-66512	5497.92	7914.88	9969.96

On the other hand the thermodynamic parameters for adsorption on PANI alone have opposite signs indicating that the adsorption is not very much favorable.

Conclusion

The present study suggested that $NiFe_2O_4$-PANI is a promising and effective nanocomposite for the removal of As(III) from water containing arsenic. The process of adsorption was found to depend significantly on the *p*H of the solution. At *p*H 8, maximum adsorption occurred. The process was found to follow the Langmuir isotherm and pseudo 2^{nd} order rate kinetics. The dimensionless separation factor calculated from the Langmuir constants confirmed favorable adsorption of As(III) on $NiFe_2O_4$-PANI nanocomposite. The process was found thermodynamically feasible as shown by negative free energy change and positive entropy change. It is concluded that $NiFe_2O_4$-PANI nanocomposite is an effective adsorbent for the removal of arsenic from water solutions.

References

1 Chris L X, Yalcin S & Mingsheng M, *Environ. Sci. Technol*, 34 (2000) 2342.
2 Pan Y F, Chiou C T & Lin T F, *Environ. Sci. Poll Res*, 17 (2010)1401.
3 Urbano B F, Villenas I, Bernabé L R & Cristian H C, *Chem Eng J*, 268 (2015) 362
4 Mohan D & Charles P, *J Hazard Mater*, 142 (1–2) (2007) 1.
5 Salameh Y, Ahmad B A, Allen S, Walker G & Ahmad M N M, *Chem Eng J*, 259 (2015) 663.
6 Wang Y, Liu W, Wang T & Ni J, *J Colloid Interface Sci*, 440 (2015) 253.
7 Boddu V M, Abburi K, Talbott J L, Smith E D & Haasch R, *Water Res*, 42 (2008) 633.
8 IARC, Vol 1–73, 1998, (http://www.iarc. htm) (updated November 30, (1998).
9 WHO, *Exposure to Arsenic: A major public health concern*, WHO Document Production Services, Geneva, Switzerland, (2010).
10 EPA, Environmental Protection Agency, Environmental Pollution Control Alternatives, EPA/625/5-90/025, EPA/625/4-89/ 023, Cincinnati, US, (1990).
11 Maushkar M J, *Guidelines for water quality monitoring*, Central pollution control board (A Government of India organisation), Delhi, India, (2007).
12 BIS, (Bureau of Indian Standards) 10500, *Indian Standard Drinking Water Specification*; First revision, vol. 1–8, Bureau of Indian Standard Publication, New Delhi, India, (1991).
13 Hu C, Liu h, Chen G & Qu J, *Sep Purif Technol*, 86 (2012) 35.
14 Ali I, Gupta V K, Khan T A & Asim M, *Int J Electrochem Sci*, 7 (2012) 1898.
15 Yao S H, Jia Y F & Zhao S L, *Environ Technol*, 33 (2012) 983.
16 Shih M C, *Desalination*, 172 (2005) 85.
17 Awual M R, Hossain M A, Shenashen M, Yaita T, Suzuki S & Jyo A, *Environ Sci Pollut Res*, 20 (2013) 421.
18 Liu T, Yang Y, Wang Z L & Sun Y, *Chem Eng J*, 288 (2016) 739.
19 Zavareh S, Zarei M, Darvishi F & Hasan A, *Chem Eng J*, 273 (2015) 610.
20 Kumari V & Bhaumik A, *Dalton Trans*, 44 (2015) 11843.
21 Bruno F U, Villenas I , Bernabé L R & Cristian H, *Chem Eng J*, 268 (2015) 362.
22 Ma W, Meng F, Cheng Z, Xin G & Duan S, *Biores Tech*, 186 (2015) 356.
23 Önnby L, Svensson C, Mbundi L , Busquets R, Cundy A & Kirsebom H, *Sci Tot Environ*, 473-474 (2014) 207.
24 Qu X, Pedro J J A & Li Q, *Water Res*, 47 (2013) 3931.
25 Xu P, Zeng G M , Huang D L, Feng C L, Hu S, Zhao M H , Lai C, Wei Z, Huang C, Xie G X & Liu Z F, *Sci Tot Environ*, 424 (2012) 1.
26 Ali I, *Chem Rev*, 112 (2012) 5073.
27 Mostafa M G & Hoinkis J, *Int J Environ Sci, Manag Eng Res*, 1 (1), (2012) 20.
28 Hua M, Zhang S, Pan B, Zhang W, Lv L, & Zhang Q, *J Hazard Mater*, 211-212 (2012) 317.
29 Liu Z, Wang H & Liu C, *Chem Comm*, 48 (59) (2012) 7350.
30 Kooti M & Sedeh A N, *J Mater Sci Technol*, 29 (1) (2013) 34.
31 Shyaa A A, Hasan O A & Abbas A M, *J Saudi Chem Soc*, 19 (2015) 101.
32 Chitra P, Muthusamy A, Dineshkumar S , Jayaprakash R & Chandrasekar J, *J Mag Magc Mat*, 384 (2015) 204.
33 Aggrawal S & Singh N B, *Advanc Mat lett*, (Communicated).
34 Gupta V K, Agarwal S & Saleh T A, *J Hazard Mater*, 185 (2011) 17.
35 Carlos A, Carlos A F, Torras J, Meneguzzi A, Canales M, Rodrigues M A S & Casanovas J, *Polymer*, 49 (2008) 5169.
36 Costa A C F M., Leite A M D, Ferreira H S, Kiminami R H G A, Cavac S & Gama L, *J Eur Ceram Soc*, 28 (2008) 2033.
37 Abdiryim T, Xiao-Gang Z & Jamal R, *Mater Chem Phys*, 90 (2005) 367.
38 Khairy M, *Synthetic Metals*, 189 (2014) 34.
39 Choudhury A, *Sensors Actuators B*, 138 (2009) 318.
40 Stejskal J, Trchova M, Brodinova J, Kalenda P, Fedorova S V, Prokes J, Zemek J, *Colloid Interface Sci*, 298 (2006) 97.
41 Choudhury A, *Sensors Actuators B*, 138 (2009) 318.

42 Bhaumik M, Maity A, Srinivasu V V & Onyango M S, *J Hazard Mater*, 190 (2011) 381.

43 Tuutijarvi T, Lu J, Sillanpaa M & Chen G, *J Hazard Mater*, 166 (2–3) (2009) 1415.

44 Bard A J, Parsons R & Jordan J, *Standard Potentials in Aqueous Solutions* (Marcel Dekker, New York) (1985).

45 Ghimire K N, Inoue K, Makino K & Miyajima T, *Sep Sci Technol*, 37 (2002) 2785.

46 Chang Y Y, Lee S M & Yang J K, *Physicochem Eng Asp*, 346 (2009) 202.

47 Razzouki B, Hajjaji S E, Azzaoui K, Errich A, Lamhamdi A, Berrabah M & Elansari L L, *J Mater Environ Sci*, 6 (5) (2015) 144.

48 Roy P, Mondal N K, Bhattacharya S, Das B & Das K, *Appl Water Sci*, 3 (2013)293.

49 Pena M E, Korfiatis G P, Patel M, Lippincott L & Meng X G, *Water Res*, 39 (2005) 2327.

50 Li Z j, Deng S B, Yu G, Huang J & Lim V C, *Chem Eng J*, 161 (2010) 106.

51 Singh T S & Pant K K, Equilibrium, *Sep Purif Technol*, 36 (2004) 139.

52 Zhang G S, Qu J H, Liu H J, Liu R P & Wu R C, *Water Res*, 41 (2007) 1921.

53 Lenoble V, Laclautre C, Serpaud B, Deluchat V & Bollinger J C, *Sci Total Environ*, 326 (2004) 197.

54 Hristovski K D, Westerhoff P K, Crittenden J C & Olsow L W, *Environ Sci Technol*, 42 (2008) 3786.

55 Davodi B & Jahangiri M, *Synthetic Metals*, 194 (2014) 97.

56 Çiftçi Tülin Deniz & Henden Emur, *Powder Technol*, 269 (2015) 470

57 Jian M, Liu B, Zhang G, Liu R & Zhang X, *Physicochem Eng Aspects*, 465 (2015) 67.

58 Gupta A, Chauhan V S & Sankararamakrishnan N, *Water Res*, 43 (2009) 3862.

59 Carol K J R & Martinson A, *J Colloid Interface Sci*, 336 (2009) 406.

60 Luther N B S, Kim J & Parsons J G, *Microchem J*, 101 (2012) 30.

61 Zhu H, Jia Y, Wu X & Wang H, *J Hazard Mater*, 172 (2009) 1591.

62 Royer B, Cardoso N F, Lima E C, Vaghetti J C P, Simon N M, Calvete T & Veses R C, *J Hazard Mater*, 164 (2009) 1213.

63 Moussavi G & Khosravi R, *Chem Eng Res Des*, 89 (2011) 2182.

64 Tsai W T, Chang Y M, Lai C W & Lo C C, *J Colloid Interface Sci*, 289 (2005) 333.

65 Sprynskyy M, Buszewski B, Terzyk A P & Namiesnik J, *J Colloid Interface Sci*, 304 (2006) 21.

66 Crini G, *Arsenics Pigments*, 77 (2008) 415.

67 Teng H & Hsieh C, *Ind Eng Chem Res*, 37 (1998) 3618.